Functional and molecular modelling studies of two hereditary fructose intolerance-causing mutations at arginine 303 in human liver aldolase

Rita SANTAMARIA*[1], Gabriella ESPOSITO*[1], Luigi VITAGLIANO†, Vincenza RACE*, Immacolata PAGLIONICO*, Lucia ZANCAN‡, Adriana ZAGARI† and Francesco SALVATORE*[2]

*Dipartimento di Biochimica e Biotecnologie Mediche, CEINGE-Biotecnologie Avanzate, Università di Napoli 'Federico II', Via S. Pansini 5, I-80131, Napoli, Italy, †Centro di Studio di Biocristallografia, CNR, and Dipartimento di Chimica, Università di Napoli 'Federico II', Via Mezzocannone 4, I-80134 Napoli, Italy, and ‡Dipartimento di Pediatria, Università di Padova, Via Giustiniani 3, I-35128 Padova, Italy

We have identified a novel hereditary fructose intolerance mutation in the aldolase B gene (i.e. liver aldolase) that causes an arginine-to-glutamine substitution at residue 303 ($Arg^{303} \rightarrow Gln$). We previously described another mutation ($Arg^{303} \rightarrow Trp$) at the same residue. We have expressed the wild-type protein and the two mutated proteins and characterized their kinetic properties. The catalytic efficiency of protein Gln^{303} is approx. 1/100 that of the wild-type for substrates fructose 1,6-bisphosphate and fructose 1-phosphate. The Trp^{303} enzyme has a catalytic efficiency approx. 1/4800 that of the wild-type for fructose 1,6-bisphosphate; no activity was detected with fructose 1-phosphate. The mutation $Arg^{303} \rightarrow Trp$ thus substitution impairs enzyme activity more than $Arg^{303} \rightarrow Gln$. Three-dimensional models of wild-type, Trp^{303} and Gln^{303} aldolase B generated by homology-modelling techniques suggest that, because of its larger size, tryptophan exerts a greater deranging effect than glutamine on the enzyme's three-dimensional structure. Our results show that the $Arg^{303} \rightarrow Gln$ substitution is a novel mutation causing hereditary fructose intolerance and provide a functional demonstration that Arg^{303}, a conserved residue in all vertebrate aldolases, has a dominant role in substrate binding during enzyme catalysis.

Key words: homology-modelling techniques, kinetic analysis, protein expression.

INTRODUCTION

Fructoaldolases (EC 4.1.2.13) catalyse the specific and reversible cleavage of fructose 1,6-bisphosphate (FBP) and fructose 1-phosphate (F1P) into dihydroxyacetone phosphate and D-glyceraldehyde 3-phosphate or D-glyceraldehyde respectively. In vertebrates there are three genetically distinct aldolase isoenzymes, each with a distinct expression pattern: aldolase A is predominant in muscle, aldolase B in liver, kidney and small intestine, and aldolase C in the brain. Aldolases A and C are expressed constitutively, whereas the B isoenzyme is under dietary control. All the functional enzymes are homotetramers of approx. 160 kDa [1].

In humans, aldolase B deficiency causes hereditary fructose intolerance (HFI), a recessively inherited disorder of carbohydrate metabolism whose frequency is estimated to be 1 in 20000 live births [2]. The human aldolase B gene is 14,500 bp long; it consists of nine exons and encodes a 364-residue polypeptide (type B monomer). So far, 23 mutations have been identified in the aldolase B gene of patients affected by HFI [3]. They include mis-sense and nonsense mutations, large and small deletions and mutations in the splicing regions. The most common HFI mutations in Europe are $Ala^{149} \rightarrow Pro$ and $Ala^{174} \rightarrow Asp$ in exon 5, and $Asn^{334} \rightarrow Lys$ in exon 9. The other mutations are spread throughout the entire aldolase B gene; their frequencies differ between ethnic groups [3].

In recent years we have investigated the aldolase B gene of patients with clinical HFI symptoms and identified, in addition to known molecular defects, three novel disease-causing mutations [4–6]. We now describe a novel HFI mutation at Arg^{303} ($Arg^{303} \rightarrow Gln$) in the aldolase B gene. We have analysed the kinetic properties of the wild-type and of the aldolase B variants ($Arg^{303} \rightarrow Gln$ and $Arg^{303} \rightarrow Trp$) and the functional effects of these mutations on protein folding and structure. The kinetic parameters obtained reflect the altered molecular structures derived by homology-modelling techniques.

EXPERIMENTAL

Materials

Restriction endonucleases were purchased from New England Biolabs. *Taq* polymerase, T4 DNA ligase, isopropyl β-D-thiogalactoside (IPTG), ampicillin, PMSF and α-glycerol-phosphate dehydrogenase/triose phosphate isomerase (GDH/TIM) were purchased from Roche Molecular Biochemicals. Imidazole, FBP, F1P and NADH were purchased from Sigma-Aldrich. The pET-16b vector and the *Escherichia coli* strains BL21(DE3) were purchased from Novagen.

The patient

The proband is an Italian infant girl in whom HFI was suspected because of clinical symptoms and liver failure after the administration of sucrose-containing medicine during a feverish episode. Both parents are healthy.

DNA analysis

Genomic DNA was purified from peripheral blood leucocytes by the NaCl extraction method [7]. The whole aldolase B coding region, the splice junctions and the promoter region were

Abbreviations used: FBP, fructose 1,6-bisphosphate; F1P, fructose 1-phosphate; GDH/TIM, α-glycerol-phosphate dehydrogenase/triose phosphate isomerase; HFI, hereditary fructose intolerance; IPTG, isopropyl β-D-thiogalactoside; rec Gln^{303}, recombinant Gln^{303} aldolase B; rec Trp^{303}, recombinant Trp^{303} aldolase B; rec WT, recombinant wild-type aldolase B.

[1] These authors contributed equally to the work.

[2] To whom correspondence should be addressed (e-mail salvator@unina.it).

amplified by PCR as described previously [4–6]. The amplified DNA fragments were analysed by single-strand conformation polymorphism analysis and sequenced with the Sequenase PCR Product Sequencing Kit (Amersham Pharmacia Biotech), in accordance with the manufacturer's instructions. For Mendelian inheritance analysis of the $Arg^{303} \rightarrow Gln$ mutation in the proband's family, the amplified DNA samples corresponding to exon 8 were digested with *Apa*I at 30 °C and the products were separated on 2 % (w/v) agarose gel.

Cloning of PCR-amplified cDNA

The full-length wild-type human aldolase B cDNA, previously cloned in the prokaryotic pAT153 vector [8], was amplified by using primers that had an extension of 10 nt containing the *Nde*I site at the 5′ end (plus primer, 5′-GGAATTC**CATATG**GCCC-ACCGATTTCCAGCC-3′) and the aldolase B termination codon TAG followed by a *Xho*I restriction site at the 3′ end (minus primer, 5′-GGAATTC**CTCGAG**CTAGTAGGTATAG-CAGGC-3′). The cDNA sequence was verified by automated sequencing. The amplified cDNA was cloned into the *Nde*I and *Xho*I sites of the bacterial expression vector pET-16b, downstream from a His-tag coding sequence. To select recombinant clones, *E. coli* XL1-Blu host cells were transformed with a vector containing the target gene. Recombinant plasmid (pET-16b/cDNA) was purified over a Qiagen column (Qiagen).

Site-directed mutagenesis

The QuickChange® site-directed mutagenesis kit (Stratagene) was used to introduce mutations into the pET-16b/cDNA construct. Mutagenesis reactions were performed with a Perkin-Elmer 9600 thermal cycler. To change the normal Arg^{303} into a Gln residue, primers 5′-GTTTCTCTTATGGACAGGCCCTG-CAGGC-3′ (sense) and 5′-GCCTGCAGGGCCTGTCCATAA-GAGAAAC-3′ (anti-sense) were designed. To change Arg^{303} into a Trp residue, the sense primer was 5′-GTTTCTCTTATG-GATGGGCCCTGCAGGC-3′ and the anti-sense primer was 5′-GCCTGCAGGGCCCATCCATAAGAGAAAC-3′. After treatment with *Dpn*I to digest the parental methylated DNA, the newly synthesized DNA was used to transform the *E. coli* XL1-Blu competent cells in accordance with the manufacturer's instructions. We selected mutated clones by PCR and direct sequencing. Recombinant mutated plasmids, pET-16b/Gln^{303} and pET-16b/Trp^{303}, were purified over a Qiagen column and their full sequences were verified by automated sequencing.

Expression and purification of the recombinant enzymes

Normal and mutated recombinant plasmids (pET-16b/cDNA, pET-16b/Gln^{303} and pET-16b/Trp^{303}) were separately transformed into the host *E. coli* B strain BL21(DE3) and grown to mid-exponential phase at 37 °C in Luria–Bertani medium supplemented with 100 μg/ml ampicillin. Expression of the corresponding proteins was induced with 1 mM IPTG. After a further 3 h of growth at 37 °C, harvested cells (approx. 1.5 g) were lysed by sonication in 10 ml of a non-denaturant lysis buffer [20 mM imidazole/300 mM NaCl/50 mM NaH_2PO_4] containing PMSF (1 mM). Lysates were centrifuged for 30 min at 10000 ***g***; soluble fractions, containing the recombinant His-tagged proteins, were mixed with 1 ml of Ni/nitrilotriacetate resin (Qiagen) for 1 h at 4 °C. The lysate/resin mixtures were loaded on a column and the flow-through was collected. The resin binding the His-tagged protein was washed twice with 4 ml of washing buffer [50 mM imidazole/300 mM NaCl/50 mM NaH_2PO_4]; the recombinant aldolase B was eluted in eight fractions (0.5 ml each) with elution buffer [250 mM imidazole/300 mM NaCl/50 mM NaH_2PO_4]. The collected fractions were analysed by SDS/PAGE [10 % (w/v) gel] and those containing the bulk of the enzyme were pooled, dialysed against 20 mM Tris/HCl, pH 7.5, containing 50 % (v/v) glycerol, then stored at −20 °C. All purification steps were performed at 4 °C.

Aldolase B activity assays and kinetic studies

The substrate cleavage rate was determined spectrophotometrically by measuring NADH oxidation at 340 nm and 30 °C in a coupled assay with GDH/TIM and FBP or F1P as substrates [9]. Activity assays were conducted in a final volume of 1 ml containing aldolase recombinant protein, appropriate substrate concentrations, 0.2 mM NADH, 0.5 mM EDTA, 100 mM Tris/HCl, pH 7.5, and 10 μg/ml GDH/TIM. One unit of activity corresponds to the cleavage of 1 μmol of hexose substrate/min. Kinetic measures were performed in triplicate and K_m and k_{cat} values were calculated from double-reciprocal plots with the use of a least-squares method.

Protein characterization

Enzyme molecular masses were determined at 25 °C by co-fractionation (on FPLC) of the purified proteins with β-amylase (200 kDa), chicken ovalbumin (44 kDa) and carbonic anhydrase (29 kDa) on a 50 cm × 1.6 cm column of Sephadex G-200 (Amersham-Pharmacia Biotech) in 20 mM Tris/HCl, pH 7.4, with a flow rate of 0.2 ml/min. CD spectra were recorded at 25 °C with a protein concentration of 10 μM in a 10 mM phosphate buffer, pH 7.4, containing 10 % (v/v) glycerol, with a JASCO J-710A spectropolarimeter equipped with a cuvette with a 0.1 cm path length. Spectra were read from 190 to 260 nm; the reading was averaged for 5 s at each 1 nm increment.

Structural analysis

The human aldolase B structure was modelled with the X-ray crystal structure of human aldolase A (Protein Data Bank code 4ald) as the starting model [10]. There is a high sequence identity (69 %) between the two isoenzymes; there are neither deletions nor insertions and the sequence between Leu^{297} and Leu^{310} is identical. Hence this approach is highly reliable. Because the mutation site is far from any inter-subunit interface of the aldolase A tetramer, a single subunit of aldolase B was generated. The molecular graphics program O [11] was used to construct the aldolase B model. The energy of this model was subsequently minimized with the X-PLOR program [12]. With the same procedure, two other models of aldolase B were built with a Gln residue and a Trp residue in position 303.

RESULTS

DNA mutation analysis

The proband's aldolase B gene was analysed by single-strand conformation polymorphism analysis and direct sequencing. We have found only one alteration in exon 8 on only one allele with respect to the normal gene sequence, i.e. a G → A substitution at nt 11125, which changes the normal Arg^{303} into a Gln residue (Figure 1A). We next sequenced the entire coding region and splice junctions to look for other mutations in the proband's aldolase B gene. No other nucleotide change was identified and we diagnosed the subject as a carrier of this novel $Arg^{303} \rightarrow Gln$ mutation. This mutation abolishes an *Apa*I site in exon 8; we were thus able to follow the Mendelian transmission of the mutation in the proband's pedigree. Figure 1(B) shows that the

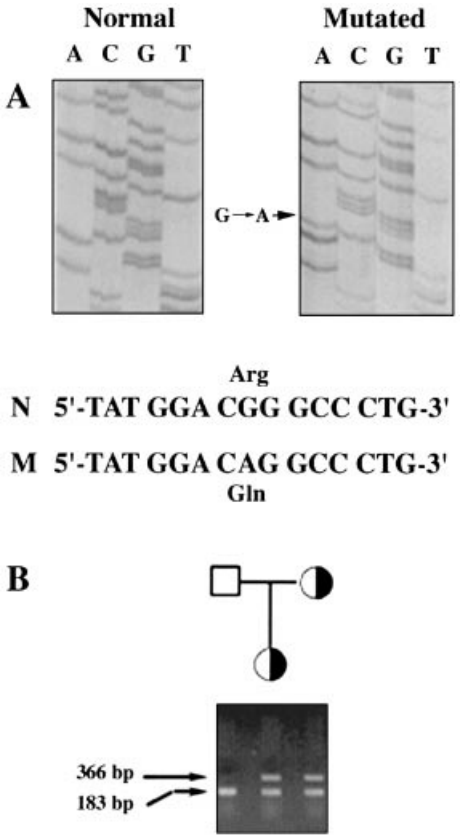

Figure 1 Identification of the Arg^{303} → Gln mutation in the human aldolase B gene

(**A**) Sequence analysis of amplified fragments spanning exon 8 from a normal (N) subject (left panel) and proband (M) (right panel). The arrow indicates the G → A transition that determines the Arg^{303} → Gln substitution. (**B**) Mendelian inheritance of the Arg^{303} → Gln mutation by restriction enzyme analysis. The lanes of the gel correspond vertically to the subjects indicated in family's pedigree. After digestion with *Apa*I, PCR products containing the normal exon 8 (366 bp) give rise to two bands, each approx. 180 bp in size (unresolved by agarose-gel electrophoresis). The pattern of a normal subject is shown in the lane corresponding to the proband's father (□). The Arg^{303} → Gln mutation abolishes the *Apa*I site (see the lanes corresponding to the proband and her mother).

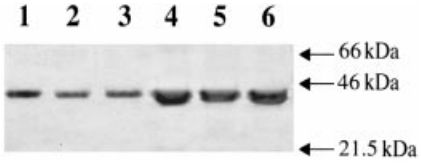

Figure 2 SDS/PAGE of human recombinant aldolase B

Lane 1, rec WT; lane 2, rec Gln^{303}; lane 3, rec Trp^{303}; lanes 4–6, as 1–3 respectively but with loadings of 10-fold more protein.

proband inherited the Arg^{303} → Gln mutation from her mother. The *Apa*I digestion of 70 chromosomes excluded the presence of the mutation in the normal population.

Expression and purification of recombinant aldolase B

To verify that the Arg^{303} → Gln mutation can cause HFI, we performed site-directed mutagenesis to produce the corresponding mutated aldolase B and to analyse its functional properties. We set up the conditions to express human aldolase B in a bacterial expression system, permitting the rapid purification of recombinant proteins under native conditions. Next we compared the activities and kinetic behaviour of the normal and mutant enzymes. We cloned aldolase B cDNA in the expression vector pET-16b, downstream from a His-tag sequence. The presence of a hexahistidine 'head' does not alter the structural or functional characteristics of aldolase B, compared with the purified liver enzyme [13]. Mutations Arg^{303} → Gln and Arg^{303} → Trp were introduced into the recombinant pET-16b/cDNA plasmid by site-directed mutagenesis. The recombinant His-tagged proteins, expressed in *E. coli* strain BL21(DE3), were recovered from the soluble fraction of the bacterial lysate and purified. The purification was checked to be more than 95% by SDS/PAGE (Figure 2). The level of expression was 10–15 mg/l of culture for the wild-type and mutated enzymes.

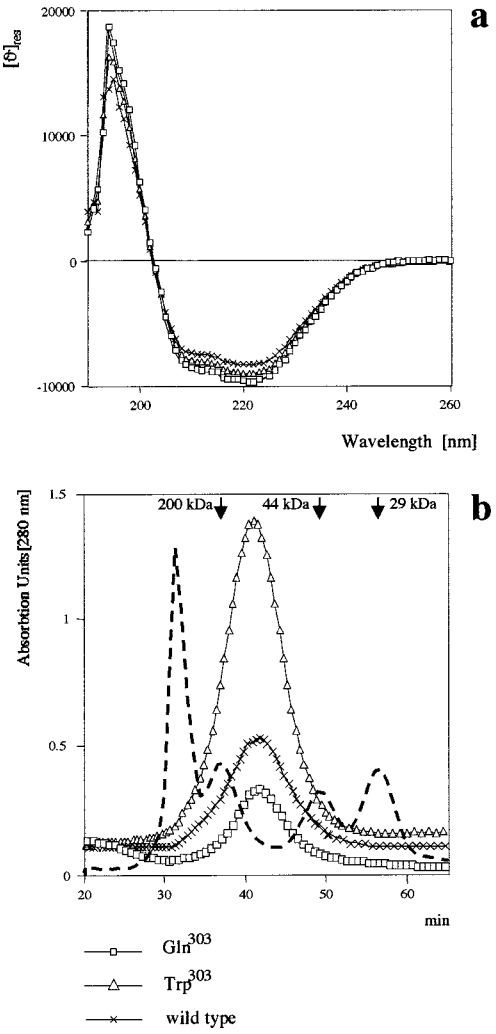

Figure 3 Structural characterization of the wild-type and Arg^{303} mutant aldolases B

(**a**) CD spectra. One spectrum is shown for each recombinant enzyme (wild-type, Gln^{303} and Trp^{303}) as indicated. Molar ellipticity per residue, $[\theta]_{res}$, is expressed as degrees · cm^2 · dmol^{-1} per residue. (**b**) FPLC profiles. The elution profiles indicate that all the recombinant enzymes have a molecular mass of approx. 170 kDa, as expected for the histidine-tagged homotetrameric form of aldolase B. The dotted line and arrows indicate the molecular masses of the protein standards used in the calibration (see the Experimental section).

Table 1 Functional characterization of the recombinant aldolase B enzymes

Results for human liver aldolase B are from [13]. Specific activity and K_m determinations were performed in triplicate on each recombinant enzyme. Abbreviation: n.d. not determined.

	Specific activity (μmol min^{-1} mg^{-1})		K_m		k_{cat} (s^{-1})		k_{cat}/K_m		Fold variance	
Protein	FBP	F1P	FBP (μM)	F1P (mM)	FBP	F1P	FBP (μM$^{-1}\cdot$s^{-1})	F1P (mM$^{-1}\cdot$s^{-1})	FBP	F1P
Human liver aldolase B	0.82 ± 0.06	0.85 ± 0.14	1.6 ± 0.5	2.3 ± 0.3						
rec WT	0.9 ± 0.07	1.05 ± 0.10	2.3 ± 0.3	2.2 ± 0.2	0.60 ± 0.03	0.70 ± 0.03	0.25 ± 0.01	0.31 ± 0.02	–	–
rec Gln^{303}	0.47 ± 0.10	0.25 ± 0.1	147 ± 15	57.5 ± 11	0.39 ± 0.04	0.15 ± 0.02	(2.7 ± 0.2) × 10^{-3}	(2.6 ± 0.2) × 10^{-3}	93	119
rec Trp^{303}	0.10 ± 0.04	n.d.	1600 ± 600	n.d.	0.08 ± 0.02	n.d.	(5.2 ± 0.7) × 10^{-5}	n.d.	4800	n.d.

CD spectra of wild-type, Gln^{303} and Trp^{303} recombinant aldolases revealed nearly identical curves within experimental error, suggesting that the three enzymes share very similar secondary structures (Figure 3a). Moreover, the spectra were very similar to those published by Doyle and Tolan [13]: indeed, the mutations did not cause major perturbations in the enzyme secondary structure. Furthermore, the molecular mass of the recombinant enzymes, determined by FPLC, was approx. 170 kDa, in accord with the homotetrameric structure expected for His-tagged aldolase B after purification under native conditions (Figure 3b).

Kinetic analyses of normal, Arg^{303} → Gln and Arg^{303} → Trp recombinant aldolase B

Next we determined the kinetic parameters of the three recombinant enzymes (Table 1). The recombinant wild-type aldolase B (rec WT) had a specific activity and K_m values for substrates FBP and F1P similar to those reported for aldolase B purified from human liver [13].

The recombinant Gln^{303} aldolase B (rec Gln^{303}) had a specific activity for FBP of 0.47 unit/mg, i.e. approx. 50 % of that of rec WT. Its K_m was approx. 60-fold the normal value and its specific activity towards F1P was 24 % (0.25 units/mg) and the K_m was approx. 25-fold that of rec WT.

The specific activity of the recombinant Trp^{303} aldolase B (rec Trp^{303}) was approx. 10 % of that of the wild-type for FBP (0.10 unit/mg compared with 0.9 unit/mg). A higher FBP concentration was required to determine the K_m of rec Trp^{303}; K_m is therefore expressed in mM rather than in μM, at variance with the other recombinant proteins (rec WT and rec Gln^{303}); the specific activity of rec Trp^{303} for F1P was not measurable.

Although specific activity results suggest that the Arg^{303} → Gln substitution had a greater effect on F1P cleavage than on FBP cleavage, substrate affinity decreased more for FBP than for F1P. In both cases k_{cat}/K_m was approx. 1/100 of normal, indicating that the Gln^{303} mutation modified FBP and F1P cleavage to about the same extent.

In contrast, the Trp^{303} mutant kinetic study showed that the cleavage of FBP was affected less than cleavage of the specific enzyme substrate F1P. K_m was measurable only for FBP and it was higher than the K_m determined for the Gln^{303} mutant towards the same substrate. Thus it seems that the Arg^{303} → Trp substitution has a greater effect than Arg^{303} → Gln on aldolase B functionality.

Structural analysis

So far there have been no reports of the experimentally derived structure of aldolase B. To establish the structural variations in the three-dimensional structure of the enzyme induced by the mutations, we constructed a model for wild-type, Gln^{303} and Trp^{303} aldolase B by using homology-modelling techniques. As expected on the basis of the high similarity between the two enzymes, the secondary structure elements and the overall folding of aldolase A were preserved in aldolase B (Figure 4a). In fact, the root-mean-square deviation of the corresponding backbone (N, C_α, C, O) atoms of the two structures was 0.59 Å. It is noteworthy that the Arg^{303} side chain presented a different orientation owing to the proximity in aldolase B of the side chain of Arg^{45} (Ser in aldolase A). This indicated a rather high flexibility of the Arg^{303} side chain. The analysis of the unbound aldolase B models carrying the Arg^{303} mutations showed that the side chain of a Gln residue and of a Trp residue could be accommodated at this position with minor modifications of the local structure of the protein. Comparison of these two mutant models with the structure of aldolase A complexed with FBP [10] reveals that the bulky Trp side chain occupied the 1-phosphate-binding site (Figure 4b), whereas the smaller side chain of the Gln residue, located in approximately the same region, left the 1-phosphate site more available for binding of the substrate (Figure 4c).

DISCUSSION

The molecular diagnosis performed in two subjects suspected of having HFI led us to identify two distinct aldolase B mutations at the level of residue Arg^{303}. In a first study we identified a point mutation that transformed Arg^{303} into Trp [5]. In the patient, who was homozygous for the mutation, aldolase B activity was not detectable in liver biopsy with either enzyme substrate. In the present study we analysed the aldolase B gene of an infant girl in whom HFI was suspected and we highlighted a nucleotide substitution that replaced Arg^{303} with a Glu residue. No other mutations were found in the gene, so that the subject was diagnosed as a carrier of HFI; the molecular diagnosis was confirmed by a subsequent fructose challenge.

The aim of this study was to shed light on how these two naturally occurring substitutions in the critical Arg^{303} residue of aldolase B affect the enzyme function, and if structural models can explain differences in their function.

We obtained the mis-sense aldolase B variants corresponding to the Arg^{303} → Gln and Arg^{303} → Trp substitutions by site-directed mutagenesis and expression in a prokaryotic host. The functional assays of rec Gln^{303} showed a residual activity for both substrates tested. Enzyme catalytic efficiencies (k_{cat}/K_m) indicated a decrease to 1/100 compared with the wild-type enzyme for both substrates.

The rec Trp^{303} protein is inactive towards the specific substrate F1P, with a low residual activity towards FBP: the catalytic

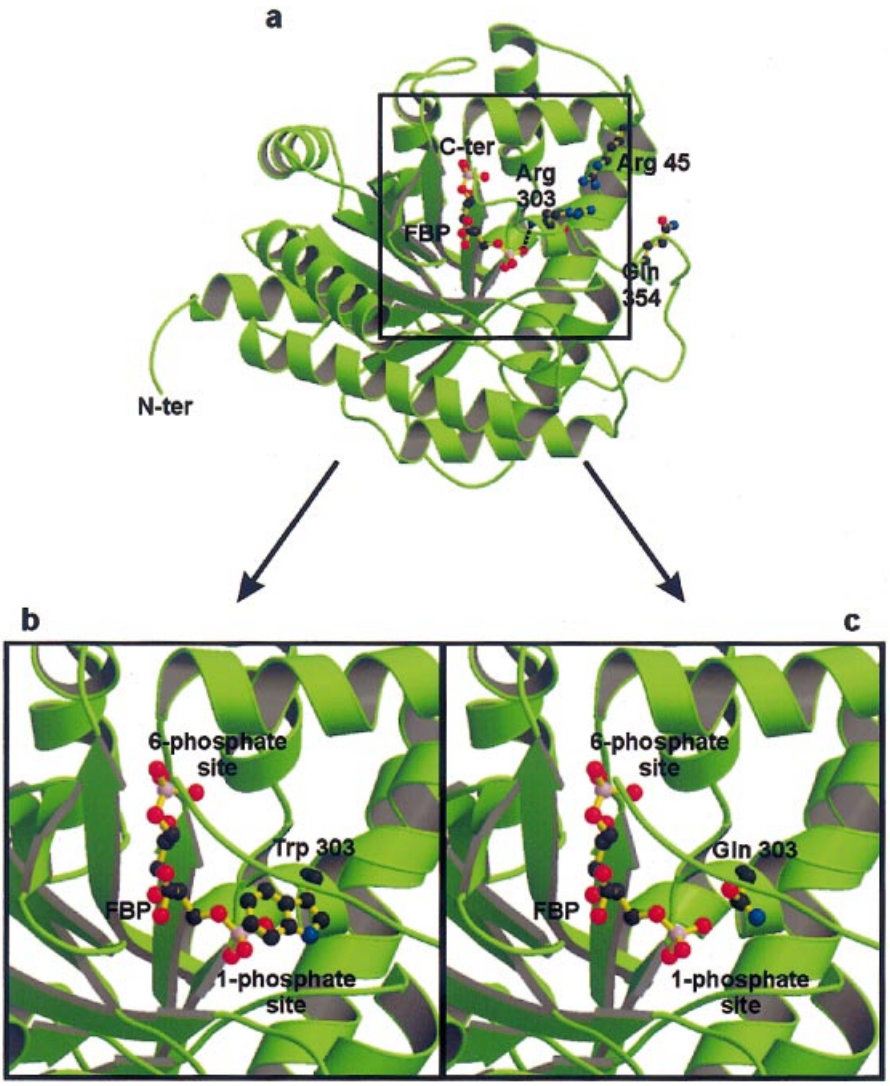

Figure 4 Ribbon diagrams of an aldolase B subunit complexed with FBP

The $(\alpha/\beta)_8$ fold is shown with α helices and β strands as coiled ribbon and flattened arrows respectively. The active site lies inside the β barrel and contains an FBP molecule. (**a**) Wild-type monomer. Only selected residues, Arg^{45}, Arg^{303} and Gln^{354}, are shown. The N, C_α and O backbone atoms of Arg^{45} and Gln^{354} have been omitted for clarity. Arg^{303} is located in the last α helix. The hydrogen bond between the 1-phosphate moiety of FBP and the backbone N atom of Arg^{303} is represented by a dotted line. The C-terminal arm is a flexible loop, which covers the active-site cavity. (**b**) Detail of the Trp^{303} enzyme active site model, with FBP and the Trp side chain drawn in ball-and-stick form. Note that the bulky side chain of tryptophan invades the 1-phosphate-binding site. (**c**) Detail of the Gln^{303} variant active-site model. FBP and the Gln side chain are shown in ball-and-stick form. Their relative positions are sterically compatible.

efficiency towards the latter substrate is approx. 4800-fold lower than wild-type. This result is consistent with the lack of aldolase B activity in liver biopsy samples from a patient with HFI homozygous for the mutation $Arg^{303} \rightarrow Trp$ [5].

Therefore functional parameters have demonstrated that two natural mis-sense mutations in aldolase B at Arg^{303} severely affect the enzyme's catalytic efficiency towards both its substrates, and that replacement with a tryptophan residue impairs the enzyme function to a greater extent than that with a glutamine residue. Furthermore, we demonstrate that the deleterious effects exerted on enzyme functionality occur with the aldolase-B-specific substrate F1P, thus explaining the HFI phenotype.

Arg^{303} is located on the α-helix that precedes the C-terminal tail; several crystal structures determined over the years have added new insights into its role in the catalysis of class I aldolases. First, a refinement of the structure of human aldolase A at a resolution of 2.0 Å showed Arg^{303} to be near the active site [14]. In the crystal structure of rabbit aldolase A determined by Blom and Sygush [15], a molecule of dihydroxyacetone phosphate, the product of the reaction, was bound to two subunits of the tetramer. This structure revealed that the Arg^{303} main chain is close to the 1-phosphate site. In addition, the Arg^{303} side chain adopts different conformations: indeed, in one subunit, Arg^{303} forms a salt bridge with Glu^{354}. Consequently, on the basis of this finding, Arg^{303} was implicated in the pathway of product release [15]. Furthermore, the structure of aldolase A complexed with FBP confirmed that the Arg^{303} backbone nitrogen atom forms a hydrogen bond with one of the oxygens of the 1-phosphate group [10]: no interaction of the Arg^{303} side chain with the substrate was found. In contrast, the structure of the complex of the aldolase A mutant $Lys^{146} \rightarrow Ala$ with FBP, although confirming that Arg^{303} backbone is close to the 1-phosphate site, shows that the Arg^{303} side chain interacts with the 6-phosphate site [16].

To explain the kinetics of the recombinant proteins, which indicate Arg^{303} to be an important residue for substrate binding,

we extrapolated the known structure of aldolase A to aldolase B and constructed a three-dimensional model of aldolase B by using homology-modelling techniques. Before analysing these data, it is worth recalling that other aldolase B gene mutations lead to changes in the V_{max} and K_m of the enzymes for both its substrates [2]. Regardless of the mutation that causes the disease, such changes resemble those observed in the present study. The overall picture emerging from the homology-modelling technique indicates that the secondary structure elements and the whole architecture of the active site, including Arg^{303}, are conserved; particularly striking is the local sequence identity from Leu^{297} to Leu^{310}, even though some structural variations have been observed. In fact, our aldolase B model shows that the proximity of the positively charged Arg^{45} (a Ser in aldolase A) to Arg^{303} can restrict its conformational freedom. As a result, the binding of the negatively charged substrates in aldolases A and B might be different. This observation is supported by the analysis of the aldolase isoenzyme sequences. Arg^{45} is a conserved residue in aldolase B from various species, whereas it is Ser in aldolase A and Gln in aldolase C; both exhibit different substrate specificities. It is noteworthy that in the aldolase B sequence, the residue in position 354 is Gln. Consequently, the strong salt bridge between Arg^{303} and Glu^{354} observed in aldolase A cannot be formed in aldolase B, a finding that does not corroborate the role of Arg^{303} in the release of the reaction products [15]. In principle, the different substrate specificity of aldolases A and B could be invoked to postulate that Arg^{303} might have a different role in the two isoenzymes. However, this possibility is weakened by the observation that residue 354 is Gln also in aldolase C, which is endowed with the same substrate specificity as aldolase A.

Computer-generated models representing Gln^{303} and Trp^{303} aldolase B yield interesting insights into the structural bases of their altered functionality. Because we recovered the recombinant mutated enzymes as native tetramers at physiological temperature (37 °C), it is difficult to attribute the observed functional impairment to folding alterations that provoke changes in their quaternary structure.

In fact, in both cases the new side chains can be accommodated in the three-dimensional model of the unbound enzyme with minor structural alterations. However, owing to the vicinity of residue 303 to the active site, the Trp side chain hinders 1-phosphate binding. Therefore it is not surprising that the activity of the Trp^{303} mutant towards F1P is not detectable. In contrast, the residual (but significant) activity exhibited by Trp^{303} towards FBP can be explained by assuming that the 6-phosphate binding site acts as the anchoring point of the substrate.

Because of the smaller steric hindrance of 1-phosphate site in the Gln^{303} enzyme, the significant increase in the K_m of the mutant towards both substrates demonstrates that the positively charged side chain of the arginine residue is important for the correct binding of the substrate. It is noteworthy that K_m increases more for FBP (64-fold) than for F1P (26-fold).

The experiments on substrate binding alterations based on the kinetics of the purified recombinant enzymes demonstrate that the mutated proteins are indeed less active than the native counterpart (see Table 1). This is borne out by a body of evidence. Choi et al. [16], for example, demonstrated for the $Lys^{146} \rightarrow Ala$ aldolase A mutant that Arg^{303} interacts with C-6-phosphate and with the sugar carbonyl group of FBP. Transformation of Arg^{303} to Ala by site-directed mutagenesis in aldolase A and determination of the kinetic constants of this mutant showed that the $Arg^{303} \rightarrow Ala$ mutation has a considerable effect on the K_m for FBP and for F1P. This effect is comparable to similar mutations at other residues implicated in binding, e.g. $Lys^{107} \rightarrow Ala$ and $Arg^{148} \rightarrow Ala$ [17], strongly suggesting that Arg^{303} also has a critical role in substrate binding of aldolase A.

It is noteworthy that the decrease in k_{cat}/K_m for FBP observed for Gln^{303} and Trp^{303} aldolase B goes in the same direction as that for the Ala^{303} aldolase A mutant analysed by Choi et al. [16]. The conclusion is that Arg^{303} has a critical role in the substrate binding of both aldolase A or aldolase B. The high sequence similarity between the two isoenzymes in this region supports the conclusion.

We thank Dr C. Pedone for CD spectra, and Jean Ann Gilder for critical reading of the text before submission. This work was supported by grants from Ministero dell'Università e della Ricerca Scientifica (PRIN 1997) and CNR (Target Project 'Biotechnology' and 'Biologia Strutturale'), Rome; Regione Campania 'Ricerca Sanitaria Finalizzata' and 'Agen-Sud', Rome, Italy.

REFERENCES

1 Salvatore, F., Izzo, P. and Paolella, G. (1986) Aldolase gene and protein families: structure, expression and pathophysiology. in Horizons in Biochemistry and Biophysics (Blasi, F., ed.), vol. 8, pp. 611–665, John Wiley and Sons
2 Gitzelmann, R., Steinmann, B. and Van den Berghe, G. (1995) Disorders of fructose metabolism. in The Metabolic and Molecular Bases of Inherited Disease, 7th edn (Scriver, C. R., Beaudet, A. L., Sly, W. S. and Walle, D., eds), pp. 905–934, McGraw-Hill, New York
3 Ali, M., Rellos, P. and Cox, T. (1998) Hereditary fructose intolerance. J. Med. Genet. **35**, 353–365
4 Santamaria, R., Scarano, M. I., Esposito, G., Chiandetti, L., Izzo, P. and Salvatore, F. (1993) The molecular basis of hereditary fructose intolerance in Italian children. Eur. J. Clin. Chem. Clin. Biochem. **31**, 675–678
5 Santamaria, R., Tamasi, S., Del Piano, G., Sebastio, G., Andria, G., Borrone, C., Faldella, G., Izzo, P. and Salvatore, F. (1996) Molecular basis of hereditary fructose intolerance in Italy: identification of two novel mutations in the aldolase B gene. J. Med. Genet. **33**, 786–788
6 Santamaria, R., Vitagliano, L., Tamasi, S., Izzo, P., Zancan, L., Zagari, A. and Salvatore, F. (1999) Novel six-nucleotide deletion in the hepatic fructose-1,6-bisphosphate aldolase gene in a patient with hereditary fructose intolerance and enzyme structure–function implications. Eur. J. Hum. Genet. **7**, 409–414
7 Miller, S. A., Dykes, D. D. and Polesky, H. F. (1988) A simple salting out procedure for extracting DNA from human nucleated cells. Nucleic Acids Res. **16**, 1215
8 Paolella, G., Santamaria, R., Izzo, P., Costanzo, P. and Salvatore, F. (1984) Isolation and nucleotide sequence of a full-length cDNA coding for aldolase B from human liver. Nucleic Acids Res. **12**, 7401–7410
9 Morris, A. J. and Tolan, D. R. (1993) Site-directed mutagenesis identifies aspartate 33 as a previously unidentified critical residue in the catalytic mechanism of rabbit aldolase A. J. Biol. Chem. **268**, 1095–1110
10 Dalby, A., Dauter, Z. and Littlechild, J. A. (1999) Crystal structure of human muscle aldolase complexed with fructose 1,6-bisphosphate: mechanistic implications. Protein Sci. **8**, 271–282
11 Jones, T. A., Zou, J.-Y., Cowan, S. W. and Kjeldgaard, M. (1991) Improved methods for building protein models in electron-density maps and the location of errors in these models. Acta Crystallogr. A**47**, 110–119
12 Brunger, A. T. (1992) A system for X-ray crystallography and NMR. X-PLOR v3.1 User's Guide. Yale University Press, New Haven, Connecticut
13 Doyle, S. A. and Tolan, D. R. (1995) Characterization of recombinant human aldolase B and purification by metal chelate chromatography. Biochem. Biophys. Res. Commun. **206**, 902–908
14 Gamblin, S. J., Davies, G. J., Grimes, J. M., Jackson, R. M., Littlechild, J. A. and Watson, H. C. (1991) Activity and specificity of human aldolases. J. Mol. Biol. **219**, 573–576
15 Blom, N. and Sygusch, J. (1997) Product binding and role of the C-terminal region in class I D-fructose 1,6-bisphosphate aldolase. Nat. Struct. Biol. **4**, 36–39
16 Choi, K. H., Mazurkie, A. S., Morris, A. J., Utheza, D., Tolan, D. R. and Allen, K. A. (1999) Structure of a fructose-1,6-bis(phosphate) aldolase liganded to its natural substrate in a cleavage-defective mutant at 2.3 Å. Biochemistry **38**, 12655–12664
17 Wang, J., Morris, A. J., Tolan, D. R. and Pagliaro, L. (1996) The molecular nature of the F-actin binding activity of aldolase revealed with site-directed mutants. J. Mol. Biol. **12**, 6861–6865

Received 8 March 2000/13 June 2000; accepted 30 June 2000